A Cooling System Using Wickless Heat Pipes for Multichip Modules: Experiment and Analysis

S. H. Rhi,* W. T. Kim and Y. Lee***

(Received June 8, 1996)

The present study is concerned with a cooling package system for electronic components such as multichip modules (MCM) which are used in many electronic system. The im of the cooling capacity up to heat flux of 4 W/cm^2 was achieved. A heat flux of 4 W/cm^2 is about two to three times of the value generally accepted as the limit by forced air cooling together with heat pipes (Kishimoto et al., 1994). The data obtained from the experimental program was used to manifest the deficiency and inaccuracies of multitude of the empirical correlations for various heat transfer modes involved in the computer simulation of the proposed system. The dominant role of the temperature distributions in the system and the related two-phase flow heat transfer have been quantitatively identified and the limit of the computer simulation for such system as proposed in the present study has been advanced.

Key Words: Thermosyphons, Cooling, Electronic Components, Multichip Modules, Simulation, Boiling, Condensation

Nomenclature

A : Surface area (m^2)
Ar : Archimedes number, Ar $=[gl_e^3(\rho_l-\rho_v)]/(\nu_l^2\rho_l)$
Bo : Bond number, $\sigma/[g(\rho_l-\rho_g)\delta_w^2]$
k : Thermal conductivity ($W/m\ K$)
c_p : Specific heat ($J/kg\ K$)
C_{SF} : Constant depending on surface finish and fluid, Eq. A.1 in Appendix
d : Inner diameter (m)
D : Outer diameter of tube (m)
Exp : Experimental
Fr : Froude numgber, Fr$=(w_{lw}^2\ \rho_l)/[gl_{ev}(\rho_l-\rho_v)]$
f_{wave} : $f_{wave}=1.15/[1-0.63(P/P_{cr})]^{3.3}$, Eq. B.3 in Appendix
g : Acceleration due to gravity (m/s^2)
h : Heat transfer coefficient ($W/m^2\ K$)
h_{LG} : Latent heat of vaporization (J/kg)
l : Length (m)
L^+ : l_c/l_e
m : $[(2h_{conv})/(k_{fin}\delta_{fin})]^{1/2}$
M : Molecular weight
Nu : Nusselt number
P : Pressure (Pascal)
Pa : Atmospheric pressure (Pascal)
P_r : P/P_{cr}
Pr : Prandtl number
P_t : Tube pitch (m)
Q : Heat transfer rate (W)
q : Heat flux (W/cm^2)
r : Radius (m)
R : Resistance (K/W)
Ra : Rayleigh number
Re : Reynolds number
Re_φ : Re$_\varphi=Q/(\pi dh_{LG}\mu_l)$
Rp : Roughness parameter
$Sim.$: Simulation
T : Temperature (℃)
TCT : Two-phase closed thermosyphon
ΔT_T : Total temperature difference between hot and cold sections
u : Velocity (m/s)
U : Overall heat transfer coefficient ($W/m^2\ K$)

* Department of Mechanical Engineering, University of Ottawa, Ottawa, Ontario, Canada KIN 6N5
** Electronic Packaging Section, Electronics and Telecommunications Research Institute (ETRI), Taejon, Korea 305-600

V : Volume (m^3)
V^+ : Dimensionless volume ratio of working fluid, V_l/V_e
WF : Working fluid

Subscripts

air : Surrounding air
b : Bare tube in the transportation zone
c : Condenser section or condensation
conv : Convection
cr : Critical
e : Evaporator section or heated zone
f : Forced
fil : Filler
free : Free or natural
g : Vapor
h : Heater
i : Inner
l : Liquid
lam : Laminar
max : Maximum
p : Liquid pool
pl : Holding plate of evaporator
s : Saturation
T : Total
t : Test tube
turb : Turbulence
w : Wall
∞ : Stream

Superscript

s : 1.0 for water and 1.7 for other liquids, Eq.A.1 in Appendix

Greek Letters

η : Efficiency
η_T : $\eta_T = 1-(A_T/A_f)/(1-\eta_f)$
δ : Thickness (m)
μ : Dynamic viscosity ($kg/s \cdot m$)
ρ : Density (kg/m^3)
σ : Surface tension (N/m)
Ψ : Parameter according to the fin shape

1. Introduction

The thermal management for electronic and electrical elements has become an important and serious issue with the rapid increase of microchip power and power densities. The need for greater speed and power with electronic devices has given rise to continuous increase in the circuit densities and power dissipation of the most advanced design chips found in the integrated electronic packages. However, these modern electrical and electronic elements with their compact sizes and powerful capabilities release a large amount of heat. The heat fluxes can be one or two orders of magnitude higher than those handled by the conventional cooling systems, and beyond the capacity of the high-performance air cooling systems.

One such example is the multichip modules (MCM) used in asynchronous transfer mode (ATM) switching systems being developed. The high packaging density of MCM decreases signal propagation delay, thus simplifies synchronization between links, reduces inductance as well as electromagnetic emission. On the other hand, the power (heat) density generated by MCM is much greater than those of conventional systems, due to the higher device operation speed and higher packaging density, and the resulting heat flux is known to be 1 to 2 W/cm^2 Which are one or two orders of magnitude higher than those of conventional systems, and beyond the capacity of the high-performance air cooling systems (Kishimoto et al., 1994). Immersion or direct liquid cooling is an alternative solution (Nelson et al., 1994), but this in turn introduces new problems because of direct contact of the electronic components with liquid.

A cooling system which can deal with such high heat flux is the one that employs two-phase closed thermosyphons (TCT)(i.e., wickless heat pipes) which combine the advantages of the traditional conventional air cooling systems with the advantages of fluid cooling, utilizing the phase change heat transfer of a working fluid. For the present objective, a two-phase closed thermosyphon is used as a high efficiency autonomous heat transferring device which removes the heat from the MCM, transfers the heat over sme distance and dissipates it to the surrounding air.

1.1 Two-phase closed thermosyphons

It has been known that very effective heat transfer and be obtained by means of evaporation and condensation of the working fluid. Heat pipes and two-phase closed thermosyphons are closed systems that utilize these processes. Both systems are very similar in terms of the functions that transport and distribute a large amount of heat by means of evaporation and condensation of the working fluid with a very mechanism of the condensate return. A two-phase closed thermosyphon (TCT) depends on the gravity, whereas a heat pipe employs capillary force for the condensate return to the evaporator. Therefore, the TCT is ineffective in the absence of the gravity force or where the condensate has to be returned to the evaporation section against gravity.

The TCT is a simple tube which contains small amount of working fluid inside. When the heat is applied to the lower section of the tube, some of the liquid vaporizes, rises toward the upper section and condensates when the temperature of the uper end is lower than the saturation temperature of the vapor. The condensed liquid comes down along the surface of the tube wall due to the gravitational force. On the other hand, the heat pipe has a wick struture inside wall. This wick provides a capillary force for the condensed liquid even against the gravity. TCTs are sometimes referred as wickless heat pipes or gravity assisted heat pipes.

The major difference between the two-phase closed thermosyphons used in the present study and the conventional two-phase closed thermosyphons is that the former has very long transport zone (adiabatic zone) between the evaporator and condenser sections which dictates that the previous experimental results on the conventional thermosyphons can not be directly used.

1.2 Objectives of the present study

The aim of the cooling capacity of the present experimental system is to obtain the cooling heat flux of up to 4 W/cm^2 which is about two to three times of the value generally accepted as the limit by the forced air cooling with heat pipes (Kishimoto et al., 1994). The objective of the simulation code development is to provide the various capabilities under the different operating environment. The data obtained from the experimental program will also be used to manifest the deficiency and inaccuracies of multitude of empirical correlations for various heat transfer modes involved in the computer simulation of the proposed system and to stress the limit of the computer simulation for such a system as proposed in the present study.

It will be shown that a computer code alone could not give any meaningful quantitative results unless it is accompanied with some experimental results, implying that no computer code should be developed for a system such as proposed without a benchmark experimental verification.

2. Experimental

The experimental apparatus consists of the main TCT assembly, illustrated in Fig. 1, the cooling system for the condenser section, the heat generation section and the charging system.

2.1 Main TCT assembly

The test assembly shown in Fig. 1 was manufactured with ultimate cooling capacity of up to 5 W/cm^2 with the maximum surface temper-

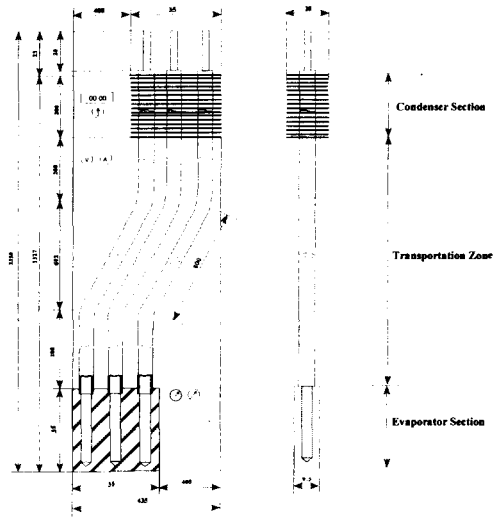

Fig. 1 Test assembly (numbers are in millimeter)

ature of the evaporator section of 75℃ and the ambient air temperature of 25℃, resulting the overall temperature difference of about 50℃. The evaporator section made of copper [35 mm×35 mm×9.5 mm (high)], illustrated as in Fig. 1, was developed based on a novel yet simple concept. The design was introduced to improve the overall thermal performance of the thermosyphon by eliminating the extra thermal resistance from the system, as well as to make the manufacturing process of the evaporator section simpler and has never been reported in the literature.

The condenser section made of brass tube with copper fins, has a dimension of 20 mm×35 mm×200 mm and a provision was made to have the exposed area of the condenser section varied. The condenser section is cooled by forced conection, using a fan. The finned condenser section was installed in a channel of 290 mm long with a cross section of 202 mm×35 mm, made of 6 mm thick transparent acrylic for the uniform air flow. For the measurement of flow velocity, a portable hot-wire probe (ANE, type Ni-125) was used. The ranges of the velocities between fins were: from 0 and up to 4.4 m/s for full cross section area and up to 6.8 m/s for the smallest cross section area.

The brass tubes for the transportation section were bent at a length of 200 mm in one direction at the angle of 150°. At the length of 800 mm, the tubes were bent again at the same 150° angle but in the opposite direction (i.e. the each part of the tubes were parallel to another and laid in one plane.) The configuration is shown in Fig. 1. This is to demonstrate that the TCTs do not have to be always straight.

To measure the temperature distribution over the length of the thermosyphons, 16 T-type thermocouples were provided along the test assembly. All thermocouples were calibrated *in situ* and connected.

2.2 Heat generation section

A special flat plate heater was designed and manufactured for the simulation of MCM operation. The heater, shown in Fig. 2, consisted of a heating element made from BeO on a ceramic sheet plate with metal as an electrical conductor

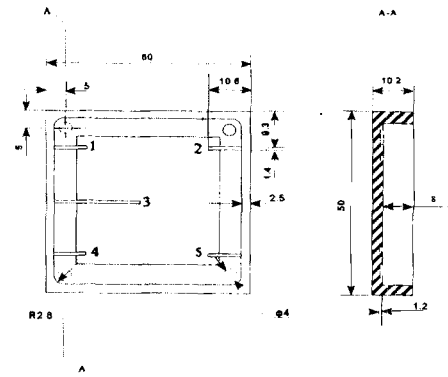

Fig. 2 Heater assembly (numbers are in millmeter)

from one side and covered with thin layer of electrical insulating material and a copper box. The heating element of 35×35 mm was installed in the copper box (50×50×10.2 mm) with the cut opening (35×35×8 mm). The opening was covered with a plate. The thickness of the copper wall facing the heating layer was 2.2 mm. Heating of the element was accomplished by an alternating current passing through the thin layer of BeO.

The power to the heater was supplied by a variable autotransformer (type 116B, input-120V, output-0-140V and up to 10A). Five T-type thermocouples were installed into the grooves provided on the inside surface of the heat transferring copper wall as illustrated in Fig. 2.

To attain a tight contact between the heater and the evaporator of the test closed two-phase thermosyphon (TCT), the wall surface of the heat generation section through which heat is transferred to the evaporator section of the TCT is covered with one component CHO-Therm T500 insulator-elastomer [Chomerics Inc., thermal conductivity-2.7 W/(mK) and thickness-0.225 mm] which is named in the present study as "the filler". The filler was made of silicone with boron nitride and was bonded to the surface. Two nylon boxes, one with the evaporation section of the TCT and the other with the heat generating section, were screwed together. Six screws situated over perimeter of the nylon boxes allowed good contact between the heater and the evaporation section of the TCT through the filler.

2.3 Working fluids and charging system

To determine the best working fluid, refrigerants R-11 and R-113, ethanol, water, acetone, FC-72 any FC-87 were tried under various conditions. Theoretically, any kind of fluids could be used as the working fluid and, water is to be the best choice by considering thermal physical properties. However, it has many other drawbacks as the working fluid of a TCT.

The charging system consisted of a vacuum pump, a McLeod gauge, vacuum valves and a special syringe to charge the desired amount of the working fluid into the test TCT.

2.4 Experimental procedure

The usual experimental procedure was employed; great care was taken to remove air and other non-condensible gases from the charging system and test thermosyphons before a new working fluid was charged and special precautions were made to remove non-condensible gases from the working fluids. The power input to the heater of the test thermosyphons was increased stepwise until a desired value of heat flux density was obtained. After each series of test with a particular working fluid, the thermosyphons and the charging system were thoroughly cleaned by repeated washing and then vacuum dried, tested for vacuum and leaks checked and corrected. After all system was evacuated, a desired amount of the new working fluid was charged into each test thermosyphon from the thermosyphon in the charging system and the next series of test was repeated. All the instruments for the measurement of various parameters have been calibrated *in situ*.

2.5 Data reduction

The tube overall heat transfer coefficient, U_T, of the test TCT for the cooling system is defined as:

$$U_T = q/(T_h - T_{air}) \quad (1)$$

The heat flux per unit area was calculate from the power measurements which was obtained from the voltmeter and ammeter coupled into the power supply circuit of the main heater. The heat losses through the insulation of the heating and evaporation section were seen negligible because of low heat flux generated in the heater and good insulation of the heating and the evaporator sections.

The temperatures in the heated section and condensing section were measured by thermocouples. The saturation temperature of the working fluid was not directly obtained. However, from the study of Lee, et al., we can assume the temperature measured by the thermocouple installed in the middle of the transportation zone as the saturation temperature.

The errors involved in the calculation of the tube heat transfer coefficient were generally due to the inaccuracy of the temperature and power measurements. Even if the readings of the power and the temperatures were recorded after the steady state has been reached, a small fluctuation was observed ($\pm$0.2V for voltage, $\pm$0.01A for current and $\pm$0.2℃ for temperature).

3. Analysis : Simulation

Since a purely analytical solution for the proposed cooling system is not possible due to the two-phase fluid flow involved, a "lumped" resistance network method was used for the computer simulation code. The aim of the simulation code is to provide the capability to predict many variables which would affect the performance of the proposed cooling system under the different operating condition as well as many empirical correlations used in the simulation for the evaporation and condensation, and the shape factors available in the literature. The code would also identify whether the proposed design is possible based on the flooding limit calculation of the system.

3.1 Code development

A simulation computer code was developed from the following environments:

a. Program language : Microsoft Visual Basic 3.0.

b. Programming environment : Microsoft Window 3.1 or 95.

c. Working environment : Microsoft Window 3.1 or upper version.

d. Programming method : Gauss-Seidel iteration method based on the "lumped" thermal resistance network.

3.1.1 "Lumped" thermal resistance network

Under the steady-state conditions of the test, a "lumped" thermal resistance model as shown in Fig. 3 was used to estimate the heat transfer characteristics of the present experimental cooling system. Each thermal resistance between the heat generation section and the ambient can be written as:

$$R_T = 1/(UA) = \sum R_{ij} = R_{12} + R_{23} + R_{34} + R_{T47} \quad (2)$$

where

$$1/R_{T47} = 1/R_f + 1/R_n$$
$$R_f = R_{45} + R_{56} + R_{67}$$
$$R_n = R_{45}' + R_{56}' + R_{67}'$$
$$R_{12} = \delta_{fil}/(k_{fil}A_h)$$
$$R_{23} = 1/(k_{pl}S)$$
$$R_{34} = 1/(h_e \pi d l_h)$$
$$R_{45} = 1/(h_c \pi d l_c)$$
$$R_{56} = \ln(D/d)(2\pi k_t l_c)$$
$$R_{67} = 1/(h_{conv}\eta_T A_T)$$
$$R'_{45} = 1/(h_c \pi d l_b), R'_{56} = \ln(D/d)/(2\pi k_t l_b)$$
and $R'_{67} = 1/(h_{free}A)$

The thermal resistance method requires a number of empirical correlations for the various thermal resistances. Several empirical correlations for boiling, condensation, enhanced forced convection and free convection were collected and evaluated for the applicability, and they are given in Appendix. The shape factors required for R_{23} were estimated from the analytical solutions from the literature. Analytical solutions of the shape factor for two cases are also given in Appendix.

3.1.2 Thermal properties

The thermal properties of working fluids, such as density and viscosity versus saturation temperature were calculated using the generally accepted methods and approximations. These calculations were necessary because of the lack of the published data pertaining, especially, to FC-72 and FC-87. Results of calculations involving FC-72 and FC-87 when compared with a few known thermal properties showed about ±10% difference. The thermal properties of other working fluids are formulated into the empirical equations using a data regression for the temperature range of -50℃ to 150℃. The analysis of these equations for the thermal properties of each working fluid showed the difference of about ±5%.

3.1.3. Operating limits

A TCT is a high-performance heat transfer

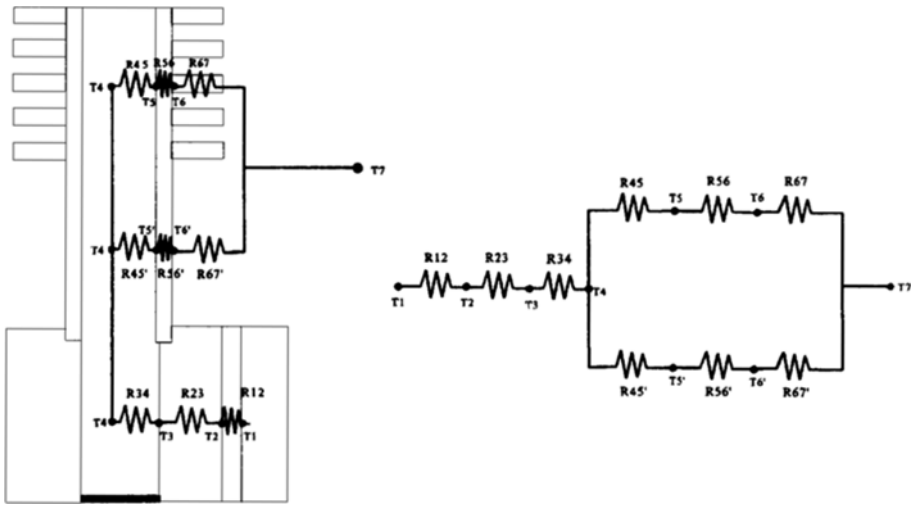

Fig. 3 Lumped thermal resistance network

device; however, when the heat transport rate is increased greatly, a limiting point may be reached where a sharp rise in walll temperature or sharp deterioration in heat transfer coefficients take place in the heating section. This performance limit can be classified into three types.

The first type performance limits occurs at very low liquid fill charges. There is a required minimum quantity of working fluid for the TCT to have a continuous circulation of vapor and condensate in accordance with the heat transport rate. If the quantity of working fluid is less than the required minimum, the returning liquid film can not cover the heating section, resulting in dry-out of the heating section and the wall temperature rises rapidly. This type is usually called the dry-out limit.

The second type is burn-out limit. Vapor bubbles are generated in the liquid pool of the evaporator section, and this nucleate boiling becomes more intense with increasing heat flux. At a certain critical radial heat flux, individual vapor bubbles are combined to form rather quickly a vapor film at the wall. This vapor film is insulating the evaporator surface from the evaporating liquid. Owing to the poor thermal conductivity of the vapor, only part of the heat input to the wall is transferred to the fluid and there is a sudden increase of the evaporator wall temperature. This limit prevails for relatively large liquid fill charges.

The third type is the flooding limit which occurs for large fill charges, high axial heat flows, but small radial evaporator heat fluxes. The high axial heat flow causes a relatively high velocity between the counter-current vapor and liquid flows, and consequently an increase of the shear stresses at the vapor/liquid interface. Thereby, large surface waves are induced at the vapor/liquid interface. Thus an instability of the liquid flow is created leading to an entrainment of liquid. The entrained liquid is transported to the condenser by the vapor flow and collected there. The high shear stresses can also cause the returning condensate flow to be completely stopped. Then the condensate flow breaks up at the flooding point. In any case, the intense entrainment or flooding causes an insufficient liquid supply to the evaporator. This leads to a local dry-out and subsequently complete dry-out of the evaporator.

An exact solution to the flooding limit is not available from the existing literature. Moreover, the present study involves a small diameter and long thermosyphon. Therefore, in the present study, the hydraulic characteristics of vapor flow is more important than the heat transfer characteristics.

Since the TCT of the present study is charged with a sufficient amount of working fluid and the heat flux is relatively moderate, the first and second types of the operating limits are not considered. Th flooding limit of the proposed system is, however, included in the code to identify whether a particular operating condition is possible or not. Wallis' correlation for the flooding velocity in vertical tubes (Wallis G.B., 1969) was used as a correlation of the flooding limit as shown in the following equation, Eq. (3).

$$j_g^{*1/2}+mj_f^{*1/2}=C \tag{3}$$

where j_g^* and j_f^* are dimensionless superficial velocities of the gas and liquid and are defined as:

$$j_g^*=j_g\rho_g^{1/2}[gD(\rho_f-\rho_g)]^{-1/2}$$
$$j_f^*=j_f\rho_f^{1/2}[gD(\rho_f-\rho_g)]^{-1/2}$$

In general, m is unity and the value recommended for C lies between 0.88 and 1. In the simulation code, the value of C calculated from j_g^* and j_f^* was compared with the value 1.

3.1.4 Fin efficiency

Heat transfer from a prime surface can be increased by attaching fins or extended surfaces. Use of a finned cooling surface is particularly effective in the case where the heat tranfer coefficient between the wall and one fluid is substantially greater than the heat transfer coefficient to the other fluid.

The fin efficiency of circular or rectangular fins attached to the TCTs involves Bessel functions, which can usually be represented in tabular and graphical forms. Therefore, for the analysis and simulation, approximate, but reasonably accurate empirical expressions presented by McQuiston

and Tree (Hewitt et al., 1994) were used. They commented that the difference between two is about ±3~4%. The main equation for the fin efficiency is Eq. (4).

$$\eta_f = \frac{\tanh(m\Psi)}{m\Psi} \tag{4}$$

3.1.5 Programming

For the thermal resistance network, the following assumptions are made:

a. The system is in a steady state.
b. Each resistance field has a "lumped" surface with a uniform temperature distribution.
c. Thermal properties are constant.
d. Radiation exchanges with surroundings are negligible.

Based on these assumptions, the simulation code was programmed with the following parameters; the initial temperature of the heater, the inlet air temperature of the forced convection side with the specification of thermal resistance fields in each nodal point, and possible operation limit which can restrict the simulation result. The nodal resistances are solved by the typical Gauss-Seidel iteration method in terms of temperature and resistance (Holman, J.P, 1989).

$$T_i = \frac{\sum_j T_j/R_{ij}}{\sum_j 1/R_{ij}} \tag{5}$$

Each iteration's value of the nodal temperature T_i is calculated according to Eq. (5), using the most recent T_j. This nodal calculation is repeated till the convergence criterion is met according to:

$$|T_i^{n+1} - T_i^n| \le \varepsilon \tag{6}$$

where n is the number of iteration. In the simulation code, ε is defined as the accuracy ranging from 0.1 to 0.00001. Obviously, increasing the precision of ε will lengthen the computational time to derive the nodal temperature.

4. Results and Discussion

The overall heat transfer coefficient, U_T, depends on the dimensionless volume of the working fluid, V^+, the evaporator-condenser length ratio, L^+, the air flow velocity in the condenser section, u_{max}, the saturation temperature, T_s, The heat flux, q, and the choice of the working fluid. The effect of each of these parameters will not be discussed here because of the limited space.

Figures 4 and 5 show the heat transfer coeffi-

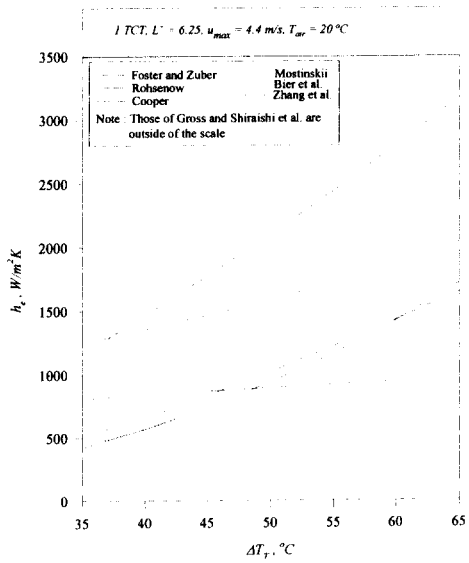

Fig. 4 h_e by different correlations with h_c of Rohsenow; WF = FC-72

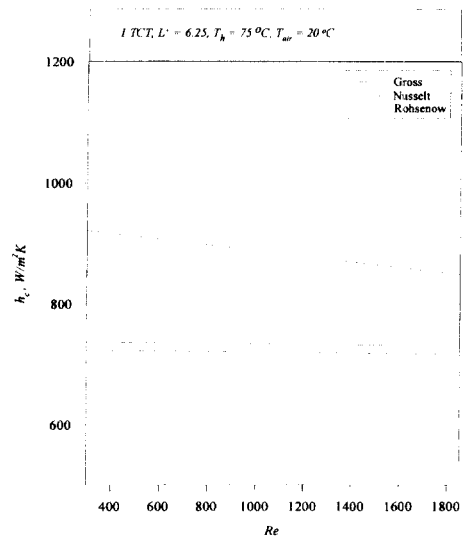

Fig. 5 h_e by different correlations with h_c of Bier et al; WF = FC-72

cients for boiling and condensation, respectively, obtained from the computer simulation using various correlations of h_e, with h_c, of Rohsenow (Fig. 4), and various correlations of h_c, with h_e, of Bier et al. (Fig. 5). Figure 6 illustrates U_T obtained by the simulation code with different h_e together with h_c of Rohsenow. As seen in the figures, each correlation generates distinct relationships.

The results with h_e's of Gross (Chen et al., 1992) and Shiraishi (Chen et al., 1992) showed much higher values than all those represented in Fig. 4. Figure 5 also shows large difference in h_c's depending on the correlation used. Therefore, Figs. 4 and 5 imply that it is necessary to find the satisfactory correlation for a given condition or, at least, some modification of the existing correlation.

In the condenser section, sixty-six rectangular fins were installed to enhance the convective heat transfer coefficient. In the simulation computer code, two types of fin (rectangular and circular with the annular base) made available to compare the heat transfer capability with different enhancing fins. In the present study, the rectangular fins with an annular base were attached to the condenser section. The simulation showed that the system having circular fins of the same area has a higher heat transfer capability than a system of the rectangular fin. In the present study, rectangular fins were used because of greater ease of fabrication and assembly.

As demonstrated in Figs. 4 to 6, it is clearly seen that a computer code alone can not give any meaningful quantitative results unless it is accompanied with some experimental results, implying that no computer code should be developed without a benchmark experimental verification.

To verify the present simulation study, the results of the simulation are compared with those from the experimental results. However, there are some parameters which the simulation study could not predict at the moment and the comparison with experimental results are not possible, e.g., the effect of the amount of the working fluid,

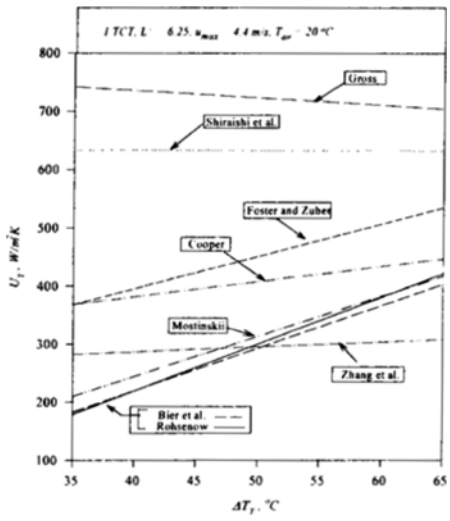

Fig. 6 U_T obtained by simulation with various correlations for h_e and h_c of Rohenow; WF=FC-72

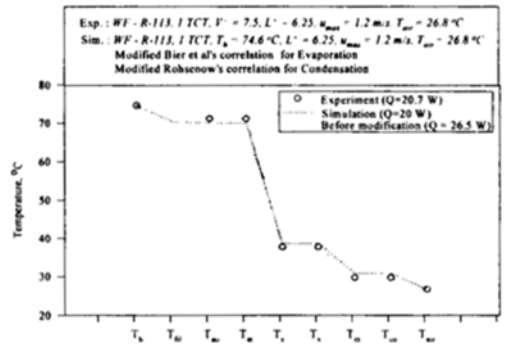

Fig. 7(a) Comparison between experiment and simulation of temperature distribution of TCT assmbly; WF=R-113

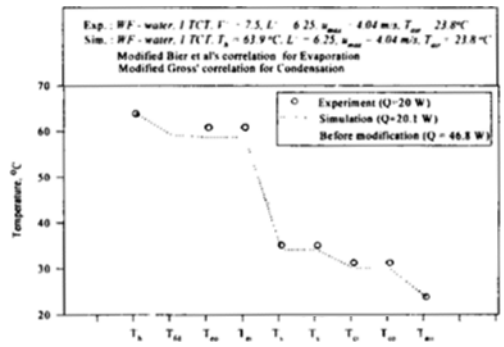

Fig. 7(b) Comparison between experimenmt and simuilation on temperature distribution of TCT assembly; WF=water

V^+, the presence of non-condensible gas in TCTs and noise level. Although these cases will not be discussed in the present paper.

Having eight empirical correlations for the boiling heat transfer coefficients, h_e, three for the condensation, h_c, three for the forced convection, h_{conv} and three for the shape factor, S, there could be as many as 216 possible solutions for a TCT under a given condition from the simulation code and every one of them could be the right one.

However, since the solution was based on the "lumped" thermal resistance network method, the key to check the correctness of the simulation code is to compare the temperature distribution within the TCT assembly obtained by the simulation with that of experiments as shown in Figs. 7(a) and 7(b).

The simulated interior temperature distributions could be quite different from the experimental results, depending on the choice of the empirical correlations used for boiling and condensation. The use of Bier et al.'s correlation for boiling (Hewitt et al., 1994) and Rohsenow' correlation for condensation (Wen et al., 1984) gave the best fit among all the correlations for the temperature distribution as seen in Fig. 7(a) for the conditions described in the figure with R-113 as the working fluid. For water as the working fluid, the use of Bier et al.'s correlation for boiling (Hewitt et al., 1994) and Gross' correlation for condensation (Gross et al., 1987) gave the best fit as seen in Fig. 7(b). However, even these combinations of boiling and condensation correlation did not give a good agreement with different working fluids. Therefore, to achieve the best fit between the experimental and simulation results, it was considered that some modification is needed for the boiling and condensation heat transfer correlations (h_e and h_c, respectively) for a particular working fluid.

To modify the given combination of the boiling and condensation heat transfer correlations, the following expression by Park was used for the heat transfer coefficients in the evaporator section and the condenser sections. The modified heat transfer coefficients for boiling and condensation (h_e and h_c) are expressed, respectively, as:

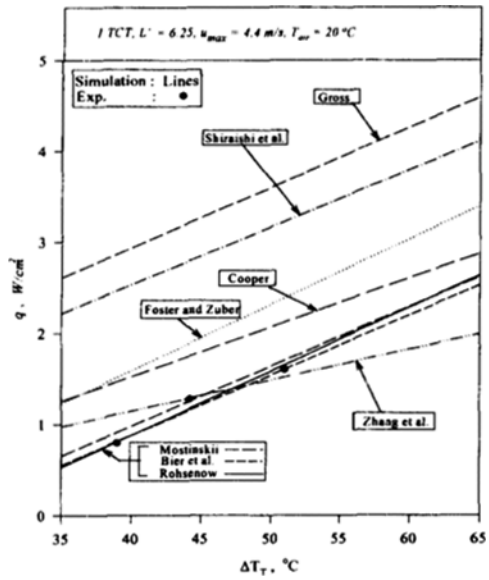

Fig. 8 Effect of ΔT_T on q with simulation by various h_e and h_c of Rohsenow; WF = FC-72

$$h_j = C_j x_j^{m_j} \quad where \quad j = e \text{ or } c \tag{7}$$

where x_j is the particulars original correlation in Appendix. The constants C_e, and C_c, and exponents m_e, and m_c were determined from the experimental data so as to correlate the data best, and the values obtained are tabulated in Ref. Rhi's.

Figures 7(a) and 7(b) show the representative comparison of the experimental results with those of simulation using the original and modified values of h_e and h_c. It can be seen that the agreement is excellent. With the modified correlations for boiling and condensation, it is now possible to compare the simulation results with the experimental results and to examine the effects of the various parameters.

In Fig. 8, the results from the simulations using the different correlations for the boiling heat transfer coefficients, h_e, with the condensation heat transfer coefficient, h_c, of Roshenow (Wen et al., 1984) are compared against those from the experiment. As stated previously, the results of every simulation could be the right one. However, it is seen in Fig. 8 that only one was able to correctly predict the phenomena, i.e., *the simula-*

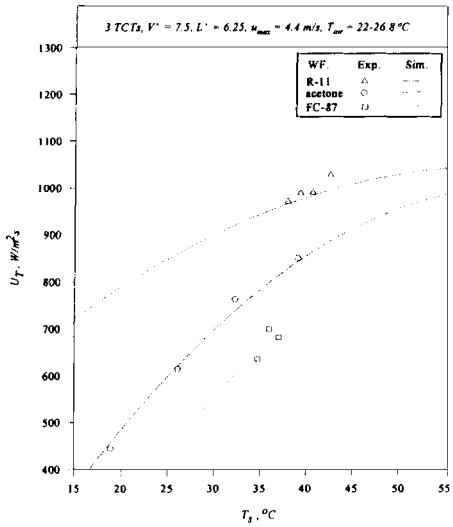

Fig. 9 Effect of T_s on U_T; WF=R-11, FC-87 and acetone

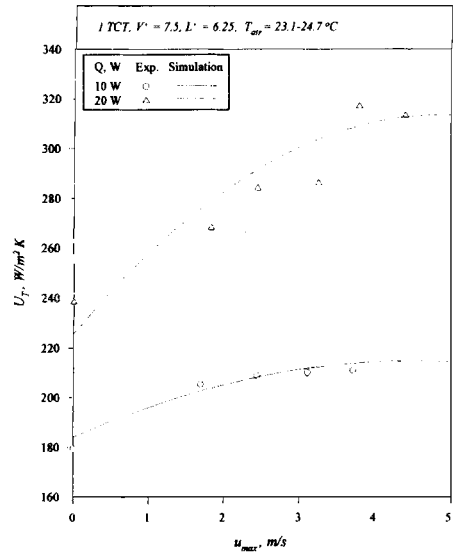

Fig. 10 Effect of u_{max} on U_T; WF=FC-72

tion with the modified correlations of Bier et al. for boiling (Hewitt et al., 1994) *and of Gross* (Gross et al., 1987) *for condensation.* Once this combination of the heat transfer coefficients for boiling and condensation were selected, the agreement between the experiment and simulation is seen very good as illustrated in Figs. 9 and 10 where the effects of the air velocity on the condenser section, u_{max} and the saturation temperature of the working fluid in the TCT, T_s, are shown, respectively.

5. Concluding Remarks

From the experimental and simulation study, the following conclusions are made:

(1) The aim of the cooling capacity up to heat flux of 4 W/cm² was achieved.

(2) The effect of non-condensible gases affect significantly the heat transfer capability of the system.

(3) The effect of heater temperature versus air velocity was identified for a given working fluid. For all working fluids, increasing the air velocity to the condenser section led to a reduced heater temperature and to an increased heat transfer capacity. The cooling air velocity to the condenser section affects the heat transfer capacity of the system.

(4) The overall heat transfer coefficient of the system was found to be increased gradually with an increasing saturation temperature.

(5) The contact resistance was seen as one of the major thermal resistances of the system.

(6) The effect of the length of the condenser section relative to the length of the evaporator section, L^+, showed a similar trend in all working fluids except with FC-72. Increasing L^+ would decrease the saturation temperature of the system.

(7) The heat transfer capability of the present system without a fan dramatically fell for the cases of the working fluids of FC-87 and acetone. In each case, the resultant temperature distribution exceeded the design limits. Although the data were not present in the paper due to the space limit, it was seen that the present cooling system, however, was still capable to handle the heat flux of up to 2 W/cm².

(8) The simulation code developed can predict correctly the heat transfer characteristics of the present cooling system, provided the simulation code used correct empirical correlations accompanied with some benchmark experiment.

References

Bejan, A., 1993, *Heat Transfer,* John, Wiley & Sons Inc., New York.

Chen, X. Q., Zhang, Z. and Ma, T., 1992, "Heat Transfer Correlation of the Evaporator Section in A Two-Phase Closed Thermosyphon" *8th IHPC,* Beijing, pp. 354~359.

Gross, U., 1992, "Reflux Condensation Heat Transfer Inside a Closed Thermosyphon," *Int. J. Heat Mass Transfer.,* Vol. 35, No. 2, pp. 279~294.

Gross, U. and Hahne, E., 1987, "Condensation Heat Transfer Inside a Closed Thermosyphon," *6th IHPC,* Grenoble, pp. 618~623.

Hewitt, G. F., Shiress, G. L. and Bott, T. R., 1994, *Process Heat Transfer.* CRC Press, London.

Holman, J. P., 1989, *Heat Transfer,* 7th ed., McGraw-Hill Book Company, New York.

Kishimoto, T. et al., 1994, "Heat Pipe Cooling Technologies for Telecom JMCM's," *Proceedings of 4th Int. Heat Pipe Symposium,* Tsukuba, pp. 132~141.

Kutateladze, S. S., 1963, *Fundamentals of Heat Transfer,* Edward arnold Ltd., New York.

Lee,Y.and Mital, U., 1972, "A Two-Phase Closed Thermosyphon," *Int. J. Heat and Mass Transfer*, Vol. 15, pp. 1695~1707.

Nelson, R. D., Sommerfeldt, S. and Bar-Cohen, A., 1994, "Thermal Performance of an Integral Immersion Cooled Multichip Module Package," *IEEE Tr. on Components, Packaging, and Manufacturing Technology, Part A,* Vol. 17, No. 3, pp. 405~412.

Park,R. J., 1992, *Two-Phase Closed Thermosyphon with Two-Fluid Mixtures,* M. A. Sc. Thesis, University of Ottawa.

Rhi, S. H., 1996, *A Cooling System Using Two-Phase Closed Thermosyphon For Telecommunication MCM: Experiment and Simulation,* M. A. Sc. Thesis, Universitry of Ottawa.

Rohsenow, W. M., 1952,"A Method of Correlating Heat Transfer for Surface of Liquids," *Trans, ASME,* Vol. 74,pp. 969~976.

Shiraishi, M., Kikuchi, K. and Yamanishi, T., 1981, "Investigation of Heat Transfer Characteristics of a Two-Phase Closed Thermosyphon," *4th IHPC,* London, pp.95~104.

Vachon, R. I., Nix, G. H.and Tanger, G. E., 1968,"Evaluation of Constants for the Rohsenow Pool-Boiling Correlation,"*J. of Heat Transfer,* Vol. 90, pp. 239~247.

Wallis, G. B., 1969, *One-Dimensional Two Phase Flow,* McGraw-Hill Book Company, New York.

Wen, Y. and Guo, S., 1984, "Experimental Heat Transfer Performance of Two Phase Tshermosyphon," *5th IHPC,*Tsukuba, pp. 43~49.

Appendix

A. Correlations for boiling heat transfer coefficient

1. Rohsenow (1952) (Rohsenow W.M., 1952)

$$\frac{c_{pl}\Delta T_s}{h_{LG}} = C_{sf}\left[\frac{q}{\mu_l h_{LG}}\sqrt{\frac{\sigma}{g(\rho_l-\rho_g)}}\right]^{0.33}\left[\frac{c_{pl}\mu_l}{k_l}\right]^{s} \quad (A.1)$$

2. Foster and Zuber (1955) (Hewitt et al, 1994)

$$h_e = 0.00122\frac{\Delta T_s^{0.24}\Delta P_s^{0.75} c_{pl}^{0.45} k_l^{0.75}}{\sigma^{0.5} h_{LG}^{0.24}\mu_l^{0.29}\rho_g^{0.24}} \quad (A.2)$$

3. Mostinskii (1963) (Hewitt et al., 1994)

$$h_e = A^* q^{0.7} F(p)$$
$$A^* = 3.596\times 10^{-5} P_{cr} 0.69$$
$$F(p) = 1.8P_r^{0.17} + 4P_r^{1.2} + 10P_r^{10} \quad (A.3)$$

4. Bier et al. (1983) (Hewitt et al., 1994)

$$h_e = A^* q^{0.7} F(p)$$
$$F(p) = 0.7 + 2P_r[4 + 1/(1-P_r)] \quad (A.4)$$

5. Cooper (1984) (Hewitt et al., 1994)

$$h_e = 55 q^{0.67} P_r^{(0.12-0.2\ \log RP)}(-\log_{10} P_r)^{-0.55} M^{-1/2} \quad (A.5)$$

6. Shiraishi (1987) (Shiraishi et a., 1981)

$$h_e = 0.32\times \frac{\rho_l^{0.65} k_l^{0.3} c_{pl}^{0.7} g^{0.2}}{h_{LG}^{0.4}\rho_g^{0.25}\mu_l^{0.1}} q^{0.4}\left[\frac{P}{P_a}\right]^{0.23} \quad (A.6)$$

7. Gross (1990) (Chen et al., 1992)

$$Nu = 4(Ar\cdot Fr^{1/2})^{1/3} Pr_l^{1/2}(Bo/10)^n$$
$$n = 1/2 \text{ for } Bo<10,\ 1/6 \text{ for } Bo>10 \quad (A.7)$$

8, Zhang et al. (1991) (Chen et al., 1992)

$$Nu=81.19\left[\frac{\rho_l}{\rho_g}\right]^{0.0756}\left[\frac{\rho_l c_{pl}}{k}\right]^{-0.0274}\left[\frac{Dq}{h_{LG}\mu_l}\right]^{0.3621} \quad (A.8)$$

B. Correlations for condensing heat transfer coefficient

1. Nusselt (1916) (Holman J.P., 1989)

$$h_c=0.943\left[\frac{k_l^3\rho_l(\rho_l-\rho_g)gh_{LG}}{\mu_l\Delta T_s l_c}\right]^{1/4} \quad (B.1)$$

2. Rohsenow (1956) (Wen et al., 1984)

$$h_c=0.943\frac{k_l}{l_c}\left[k_l^3\frac{\rho_l(\rho_l-\rho_g)g}{\mu_l\Delta T_s k_l}\cdot[h_{LG}+0.68c_{pl}\Delta T_s]\right]^{1/4} \quad (B.2)$$

3. Gross (1987) (Gross et al., 1987)

$$Nu=\sqrt{(Nu_{lam}f_{wave})^2+(Nu_{turb})^2}$$
$$Nu_{lam}=0.925(Re_\varphi)^{-1/3}$$
$$Nu_{turb}=0.021(Re_\varphi)^{+1/3} \quad (B.3)$$

C. Correlations for forced and natural convection heat transfer coefficient

1. Empirical correlations for forced convection from a finned area

a. Knudsen and Katz (1958) (Holman J.P., 1989)

$$\frac{hd}{k_f}=C\left[\frac{u_\infty d}{\nu_f}\right]^n Pr^{1/3}$$

C=0.683, n=0.466 for $40<Re<4000$ (C.1)

b. Fand (1965) (Holman J.P., 1989)

$$Nu_f=(0.35+0.65Re_f^{0.52})Pr_f^{0.3} \quad (C.2)$$

c. Churchill and Bernstein(1977) (Holman J.P., 1989)

$$Nu=0.3+\frac{0.62Re^{1/2}Pr^{1/3}}{[1+(0.4/Pr)^{2/3}]}\cdot\left[1+\left[\frac{Re}{282{,}000}\right]^{5/8}\right]^{4/5} \quad (C.3)$$

2. Empirical equations for natural convection from the transportation zone (1956) (Bejan A., 1993)

$$\overline{Nu}=\frac{4}{3}\left[\frac{7RaPr}{5(20+21Pr)}\right]^{1/4}+\frac{4(272+315Pr)l_b}{35(64+63Pr)D} \quad (C.4)$$

D. Shape factor

1. Row of pipes of equal diameter and temperature in a semi-infinite mass (Kutateladze S. S., 1963).

$$S=\frac{2\pi l_h}{\ln\left[\frac{P_t}{\pi r}\times\sinh\left[2\pi\frac{\delta_{pl}}{P_t}\right]\right]} \quad (D.1)$$

2. Row of pipes of equal diameter and temperature in a mass bounded by two parallel planes (Kutatedze S.S., 1963).

$$S=\frac{2\pi l_h}{\ln\left[\frac{P_t}{\pi r}\times\sinh\left[\pi\frac{\delta_{pl}}{P_t}\right]\right]} \quad (D.2)$$